Journal of Applied Physics

External charge compensation in etched gallium nitride measured by x-ray photoelectron spectroscopy

Cite as: J. Appl. Phys. **131**, 185301 (2022); https://doi.org/10.1063/5.0085529
Submitted: 17 January 2022 • Accepted: 19 April 2022 • Published Online: 12 May 2022

Kevin A. Hatch, Daniel C. Messina, Houqiang Fu, et al.

COLLECTIONS

Paper published as part of the special topic on Defects in Semiconductors 2022

ARTICLES YOU MAY BE INTERESTED IN

Atomic-scale investigation of implanted Mg in GaN through ultra-high-pressure annealing
Journal of Applied Physics **131**, 185701 (2022); https://doi.org/10.1063/5.0087248

Mg-doping and free-hole properties of hot-wall MOCVD GaN
Journal of Applied Physics **131**, 185704 (2022); https://doi.org/10.1063/5.0089406

Slow optical response of semi-insulating GaN film studied by terahertz emission and photoluminescence spectroscopy
Journal of Applied Physics **131**, 185706 (2022); https://doi.org/10.1063/5.0086788

Journal of Applied Physics Special Topics Open for Submissions Learn More

© 2022 Author(s).

Journal of Applied Physics ARTICLE scitation.org/journal/jap

External charge compensation in etched gallium nitride measured by x-ray photoelectron spectroscopy

Cite as: J. Appl. Phys. **131**, 185301 (2022); doi: 10.1063/5.0085529
Submitted: 17 January 2022 · Accepted: 19 April 2022 ·
Published Online: 12 May 2022

Kevin A. Hatch,[1] Daniel C. Messina,[1] Houqiang Fu,[2,3] Kai Fu,[2,4] Yuji Zhao,[2,4] and Robert J. Nemanich[1,a)]

AFFILIATIONS

[1]Department of Physics, Arizona State University, Tempe, Arizona 85287, USA
[2]School of Electrical, Computer, and Energy Engineering, Arizona State University, Tempe, Arizona 85287, USA
[3]Department of Electrical and Computer Engineering, Iowa State University, Ames, Iowa 50011, USA
[4]Department of Electrical and Computer Engineering, Rice University, Houston, Texas 77005, USA

Note: This paper is part of the Special Topic on Defects in Semiconductors.

[a)]**Author to whom correspondence should be addressed:** Robert.nemanich@asu.edu

ABSTRACT

Electronic states at GaN surfaces and at regrowth and heteroepitaxy interfaces inhibit electronic device performance. Understanding electronic state configuration at the GaN surface is, therefore, crucial for the development of GaN-based devices, which are currently of considerable interest in power electronic applications. GaN and other wurtzite III-nitrides possess large spontaneous polarization along the *c*-axis, producing a bound sheet charge at the surface, which affects the electronic state configuration through the formation of internal and external compensation charges. Defects induced by conventional plasma-based dry etching methods may inhibit the internal screening of this bound charge and thus increase the concentration of external charged states. The surface band bending of n-type Ga-face GaN (0001) was measured with x-ray photoelectron spectroscopy after inductively coupled plasma etching to investigate the impact of dry etching on external charge compensation. GaN samples were etched using inductively coupled plasma with varying rf power and a novel plasma-enhanced atomic layer etching method using an oxidation, fluorination, and ligand-exchange mechanism. The band bending varied from 0.0 to 0.8 ± 0.1 eV for the samples measured.

Published under an exclusive license by AIP Publishing. https://doi.org/10.1063/5.0085529

I. INTRODUCTION

Gallium nitride (GaN) is a wide bandgap semiconductor of considerable interest in the development of power electronics due to its superior chemical and physical properties. GaN-based devices exhibit improvements in power per unit width, energy conversion efficiency, switching frequency, and lower on-resistance over conventional Si devices.[1–3] Electronic state configuration at GaN surfaces and interfaces has been shown to greatly affect device performance, primarily in gate leakage, current collapse, and voltage breakdown.[4–6] The failure mechanisms associated with these issues are not fully understood, but studies have suggested that defect states reduce drain current and provide a pathway for rapidly increasing gate current in a reverse polarization effect.[4–6] Piezoelectric and spontaneous polarization effects have also been shown to be of great importance in GaN/AlGaN heterostructures.[1,4,7–12]

There is a fundamental difference in the band bending of wurtzite group-III nitride (III-N) surfaces when compared to Si, diamond, zinc-blende, and traditional III–V and II–VI structures, which arises from the spontaneous polarization, the bound charge at the surface and interfaces, and the compensating charged states.[4] Compensation of the bound charge arises from a combination of internal screening through the formation of a surface charge region composed of electrons and ionized donors and external screening through external surface charged states. The distribution of these compensation charges affects the internal electric field, which ultimately affects device performance.

Published under an exclusive license by AIP Publishing

Conventional dry etching techniques, such as inductively coupled plasma (ICP) etching and reactive ion etching (RIE), are essential in forming device structures. However, these etch processes are known to introduce electrically active defects, which hinder device performance.[13–20] The ion component of these methods relies on physical interactions with the surface through momentum transfer with surface atoms. This may introduce significant defect concentration in the surface and near-surface regions, as well as deeper electrically active damage, which may propagate more than 50 nm into the material.[21] Surface defects induced by these dry etch methods may inhibit internal compensation of the polarization bound charge, resulting in a larger concentration of external charged states. ICP etching allows for mitigation of defect formation through greater control of ion energy and flux, compared to RIE, by adjusting radio frequency (rf) bias and ICP power.[22–26] Several studies have found high temperature annealing and N_2 plasma treatment to be effective in the recovery of etch-induced damage with improvement in surface roughness and optical and electrical performance.[14–17,27]

Atomic layer etching (ALE) processes produce comparatively low damage as the active region is limited to surface groups and has also been proposed as a method for removing material from the surface and near-surface regions where significant defects are present.[28–31] For this study, the GaN surface is first oxidized by a remote O_2 plasma, which produces ∼1 nm of oxide at the wafer surface, as measured by x-ray photoelectron spectroscopy (XPS) and ellipsometry. Then, the oxide is fluorinated using an HF exposure. The initial plasma oxidation is necessary to provide a pathway for fluorination by HF, as Johnson *et al.* have found that HF does not sufficiently fluorinate the GaN surface for ALE.[32] Last, the fluorinated surface is removed through the formation of stable but volatile complexes through ligand exchange with trimethylgallium (TMG). A schematic of this etch process is shown in Fig. 1. Several cycles of sequential HF and TMG exposures are required between each plasma oxidation to remove the surface oxide and complete one ALE "supercycle." The use of HF and TMG thermal reactions limits the ion component of this etch method, which is expected to reduce damage to the surface and near-surface regions. This etching process and its development is discussed further by Messina *et al.*[33]

Measurements of band bending by photoelectron spectroscopy (PES) have been shown to depend on ambient conditions. Porsgaard *et al.*[34] showed that surface band bending of TiO_2 (110) varied with ambient O_2 pressure by 0.4 eV between UHV and atmospheric pressure. To remove excess adsorbates and maintain consistent surface conditions for comparison of band bending measurements, *in situ* cleaning in NH_3 at 800 °C was used to prepare surfaces. A thin surface oxide remained on all samples, which is representative of typical device interfaces.

XPS is a widely used surface characterization technique for chemical state analysis to determine chemical composition and bonding but has also been used for determination of surface band bending.[4,35–37] Band bending of GaN has shown to be of particular significance in representing surface quality after various processing methods.[4,35–40] This study compares band bending, measured by XPS, of GaN prepared by various processing methods and after various ICP etch conditions, to investigate the impact of dry etching on internal charge compensation and external charged states.

A. Polarization and bound charge in (0001) gallium nitride

The total polarization of a material is the sum of the spontaneous polarization of the equilibrium structure and the piezoelectric polarization induced by strain,

$$\vec{P} = \vec{P}_{pz} + \vec{P}_{sp}\,. \tag{1}$$

Restricting this along the *c*-axis, which is the direction of both the spontaneous polarization and in which standard bulk crystals are grown, the component of piezoelectric polarization for GaN along this direction is given by Eq. (2),

$$\vec{P}_{pz} = 2\left(\frac{a-a_0}{a_0}\right)\left(e_{31} - e_{33}\frac{C_{13}}{C_{33}}\right)\hat{c}, \tag{2}$$

where a and a_0 are lattice constants, C_{13} and C_{33} are elastic constants, and e_{31} and e_{33} are piezoelectric coefficients. The piezoelectric polarization varies between samples and depends on growth conditions, substrate material, and external temperature and pressure. Although larger than in other compound materials, the piezoelectric polarization in relaxed GaN is negligible compared to the large spontaneous polarization.[4,41,42] The crystal structure and spontaneous polarization of GaN are shown in Fig. 2.

The spontaneous polarization of wurtzite GaN has been calculated using the Berry-phase approach and local density or generalized gradient approximations to be $-0.029\ \text{C/m}^2$ for Ga-face

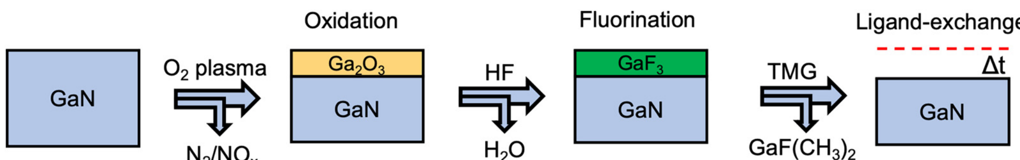

FIG. 1. Schematic of discrete reactions used in plasma-enhanced atomic layer etching (PEALE) process for GaN. Etching occurs through oxidation by O_2 plasma, followed by fluorination through HF exposure, and surface removal through a ligand-exchange with trimethylgallium (TMG). N_2 purge was used between reactions to remove reaction byproducts and an unreacted precursor.

Published under an exclusive license by AIP Publishing

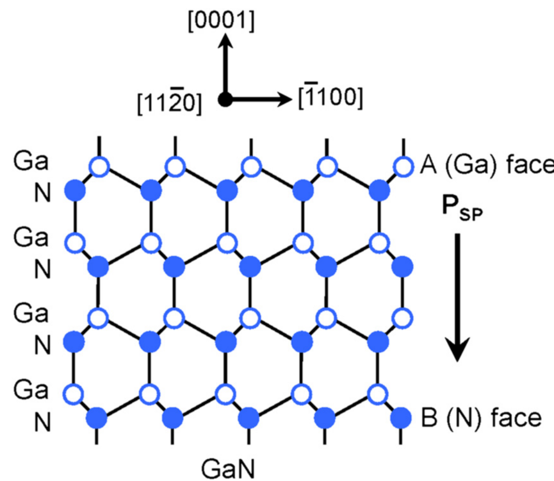

FIG. 2. Two-dimensional projection of a wurtzite GaN structure with spontaneous polarization. Reprinted with permission from Yu *et al.*, J. Vac. Sci. Technol. B **17**, 1742 (1999). Copyright 1999 American Vacuum Society.

(0001).[10,43] The polarization is directed toward the N-face (000$\bar{1}$), as shown in Fig. 1. Experimental measurements of this polarization have produced a slightly lower value than theoretically predicted. One method reported by Yan *et al.* found a polarization of approximately $-0.022\,\mathrm{C/m^2}$ using a thermodynamic model to indirectly determine the polarization from the GaN high-pressure phase transition.[44] Similarly, Lähnemann *et al.* yielded a value of $-0.022 \pm 0.007\,\mathrm{C/m^2}$ using microphotoluminescence and cathodoluminescence to determine emission energies of excitons bound to intrinsic stacking faults.[45]

This macroscopic polarization produces a negative bound sheet charge at the Ga-face (0001) as described in Eq. (3),

$$\sigma_b = \vec{P}\cdot\hat{c}, \tag{3}$$

of 1.81×10^{13} charges/cm^2, using the theoretically predicted polarization of $-0.029\,\mathrm{C/m^2}$, or 1.37×10^{13} charges/cm^2, using the experimentally measured polarization of $-0.022\,\mathrm{C/m^2}$. This study will use the theoretically predicted bound sheet charge of 1.81×10^{13} charges/cm^2 in further calculations. A corresponding positive bound sheet charge is also produced at the N-face (000$\bar{1}$).

B. Charge compensation and band bending

Gauss's law and charge neutrality require that surface charges are compensated as the internal electric field of a wide bandgap semiconductor is equal to or approximately zero. Compensation of this large bound charge at the surface arises from a combination of external screening by external charged surface states and internal screening by the formation of a space charge region, as shown in Fig. 3. The densities of these compensation charges are, therefore, inversely related.

An internal space charge region of ionized donors is formed at the surface to compensate for the bound sheet charge. Band bending is a direct consequence of this internal screening and thus provides a method to measure this internal surface screening. However, dry etching and other processing methods may introduce defects into the material, which inhibit the formation of this space charge region. The result is the formation of external charge states to compensate for the bound sheet charge.

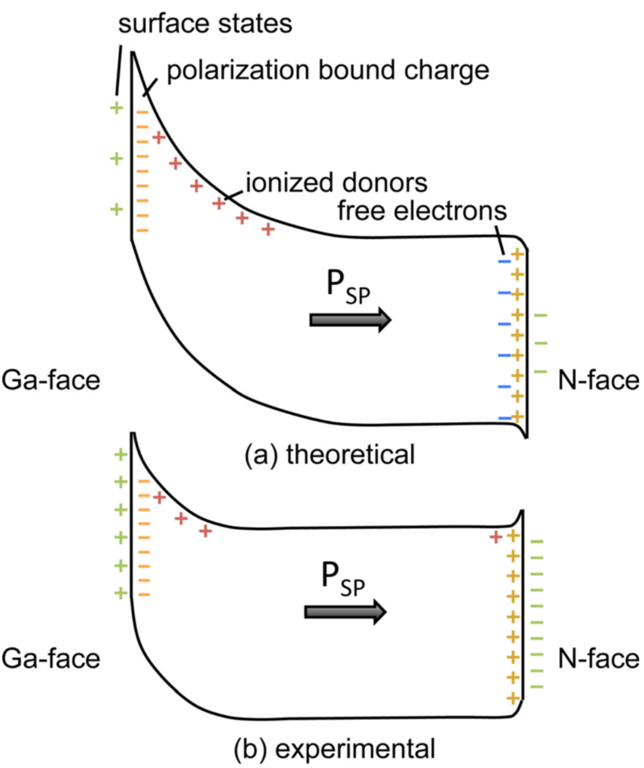

FIG. 3. (a) Theoretical and (b) experimental band bending schematic for Ga- and N-face GaN. Reprinted with permission from Eller *et al.*, J. Vac. Sci. Technol. A **31**, 050807 (2013). Copyright 2013 American Vacuum Society.

Total compensation of the bound surface charge by internal screening would require a space charge region with upward band bending much larger than the bandgap.[4] However, the large internal field results in inversion or accumulation. Band bending is, therefore, confined to the GaN bandgap, although experimental measurements on n-type GaN have been smaller, as shown in Fig. 2(b). Surface band bending of n-type GaN has been experimentally measured by various methods, including XPS,[4] UPS,[46] scanning Kelvin probe microscopy,[40] and surface potential electric force microscopy.[39] Experimental measurements of band bending in n-type GaN have yielded values ranging between −0.1 and 1.6 eV in various studies.[4,35,37,39,40,47]

Band bending is determined by the density of internal screening charge from the relation given by Eq. (4),

$$\phi_S = \frac{qN_{SS}^2}{2\epsilon\epsilon_0 N_D}, \tag{4}$$

Published under an exclusive license by AIP Publishing

where q is the electron charge, N_{SS} is the surface state density, $\epsilon = 9.5$ is the relative permittivity of GaN, $\epsilon_0 = 8.85 \times 10^{-12}$C/(V m), and $N_D = 1 \times 10^{17}$ cm^{-3} is the donor density.

It then follows that changes in the relative density of surface states may be found from band bending measurements using Eq. (5),

$$N_{SS} = \sqrt{2\epsilon\epsilon_0 N_D\left(\frac{\phi_S}{q}\right)}. \quad (5)$$

For GaN with a donor density of $N_D = 10^{17}$ cm^{-3}, this suggests that a change in a band bending of 0.1 eV, therefore, corresponds to a reduction of the surface state density by 3.2×10^{11} cm^{-2}.

The samples in this study exhibited band bending varying from 0.0 to 0.8 eV. This is in agreement with previous studies, which have found a likely Fermi level pinning state approximately 0.4–0.8 eV below the conduction band minimum.[4,46,48] This pinning state has previously been attributed to a nitrogen vacancy or a gallium dangling bond with agreement in experimental and theoretical results.[4,46,48] The band bending response to various etch and processing methods is, therefore, limited by this pinning state.

Band bending may be determined from core levels measured by XPS using a method determined by Waldrop and Grant[49] and Kraut *et al.*,[50] with the relation given in Eq. (6),

$$\phi_{BB} = (E_{CL} - E_V)_{bulk} + E_g - E_C - E_{CL,XPS}, \quad (6)$$

where E_g is the bandgap energy of GaN, taken to be 3.4 eV;[1–3] E_C is the conduction band level relative to the Fermi level, which was determined from the doping concentration (10^{17} cm^{-3}) to be 0.1 eV;[51] $(E_{CL} - E_V)_{bulk}$ is the energy spacing of the valence band from the Ga 3d core level in bulk GaN and is taken to be 17.8 eV as measured in our system and reported in previous electronic state studies of GaN (Fig. 4).[4,52–54]

The Fermi level E_F position may be determined from the doping concentration N_D of a nondegenerate semiconductor from Eq. (7),[51]

$$(E_C - E_F) = kT \ln(N_C/N_D), \quad (7)$$

where k is the Boltzmann constant and N_C is the effective density of states at the conduction band, which is 2.6×10^{18} cm^{-3} for n-type GaN. From this relation, it is estimated that the Fermi level is ~0.1 eV below the conduction band for the measured samples.

II. EXPERIMENTAL

XPS was used to study the impact of dry etching on the surface band bending and external compensation charge of GaN. XPS measurements were performed using a Scienta R3000 analyzer with a monochromatic Al Kα x-ray source (1486.6 eV) and a hemispherical detector with a pass energy of 100 eV. The system is maintained at a base pressure of 7×10^{-10} Torr and is connected to a UHV multi-chamber transfer system with a base pressure of 3×10^{-9} Torr to minimize contamination exposure between processing and characterization. Calibration of the XPS peak position was determined using a plasma cleaned gold foil. The take-off angle was 0° (from normal) for measured photoelectrons. XPS peak fitting was performed using a Gaussian–Lorentz peak shape, and a standard Shirley background was subtracted prior to spectral fitting. Using spectral fitting, measured binding energies may be resolved to ±0.1 eV. The Ga 3d, N 1s, C 1s, O 1s, and F 1s core level spectra were used for chemical state analysis at the wafer surface. Previously reported atomic sensitivity factors were used to determine surface composition.[55]

This study was performed on homoepitaxially grown GaN by metalorganic chemical vapor deposition (MOCVD) on a *c*-plane n^+-GaN substrate using trimethylgallium (TMG), NH_3, and silane (SiH_4) at a growth temperature of 1040 °C. The epitaxial GaN was *n*-type with a Si donor concentration of 10^{17} cm^{-3}. Further description of this MOCVD growth process has been published by Peri *et al.*[56] The Fermi level was determined to be ~ 0.1 eV below the conduction band at this doping density.[51]

ICP etching was performed using Cl_2 (flow rate of 30 SCCM), BCl_3 (flow rate of 8 SCCM), and Ar (flow rate of 5 SCCM) with an

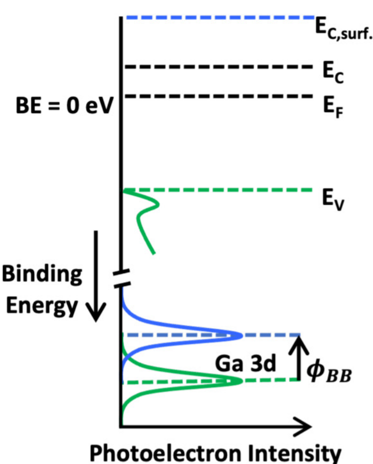

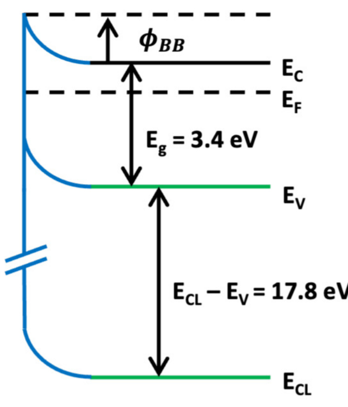

FIG. 4. GaN energy band diagram with surface band bending derived from the Ga 3d core level position measured by XPS.

Published under an exclusive license by AIP Publishing

ICP power of 400 W at a pressure of 5 mTorr. The substrates were maintained at 23 °C using He cooling during the etch process. The RF power was varied between samples from 5 to 70 W for "slow" and "rapid" ICP etch conditions, respectively. The slow ICP etch rate induced a DC bias of 21 V, while the rapid etch rate induced a 159 V DC bias, resulting in etch rates of 20 and 288 nm/min, respectively. Samples were etched for 2 min.

After etching, all samples were exposed to atmosphere during transfer to a multi-chamber system for XPS characterization and *in situ* processing. The multi-chamber system enabled sample transfer between XPS and various processing chambers at UHV (3×10^{-9} Torr) to reduce further exposure. Full process flow for samples measured is shown in Fig. 5.

Initial XPS measurements were taken for all samples prior to *in situ* processing. *In situ* cleaning methods were performed by high temperature annealing in NH_3 (Matheson Tri-gas, 99.9992%) ambient in a molecular beam epitaxy (MBE) chamber with a base pressure of $<1 \times 10^{-9}$ Torr. The GaN substrate was heated to 800 °C using a tungsten filament positioned under the back of the sample for 30 min. An NH_3 flux with a flow rate of 10 standard cubic centimeters per minute (SCCM) maintained the chamber pressure at 1×10^{-5} Torr throughout heating, annealing, and cool-down phases. NH_3 annealing has previously been reported to produce atomically clean and stoichiometric GaN.[57]

ALE was performed in a custom-built reactor using a novel method for GaN ALE using a conversion etch mechanism at a sample temperature of 300 °C. Remote radio frequency (rf) plasma was generated using a 13.56 MHz rf generator (MKS, Elite 300), a 50 Ω impedance matching network (MKS, MWH-05), and a 13-turn copper coil wound around a 32 mm diameter fused quartz tube. The quartz tube extended into the chamber to a distance ~25 cm above the wafer surface for remote plasma generation. The distance between the plasma source and the sample surface enables greater radical flux while limiting the ion component of the plasma process at the surface.[58,59] The O_2 plasma was ignited at 100 W for 20 s. The etching process was characterized by *in situ* ellipsometry using a Film Sense FS-1 multi-wavelength ellipsometer and the manufacturer supplied software (Film Sense, Desktop v. 1.15).

Precursors used in the presented ALE reactions were trimethylgallium [$Ga(CH_3)_3$, TMG] (STREM Chemicals, 97%) and hydrogen fluoride–pyridine [$(C_5H_5N)\cdot(HF)_x$, HF-P] (Alfa-Aeser, 70% HF by weight). The use of HF-P enables safe delivery of HF into the reaction chamber. The Ar carrier gas (Matheson Tri-gas, 99.9999%) at a flow rate of 5.0 SCCM was used for precursor delivery into the reaction chamber. N_2 gas (Matheson Tri-gas, 99.9999%) was used between O_2 (Matheson Tri-gas, 99.9999%) plasma and precursor exposures for 30 s to purge the chamber of reaction byproducts and unreacted precursor. "Supercycles" consisting of five sequential HF and TMG exposures were used between each O_2 plasma exposure. Experiments indicated that 5 HF/TMG subcycles were needed to remove the Ga–O surface species. The number of required exposures was determined in a separate GaN ALE study.[33]

N_2 plasma treatment was performed on select samples using a microwave electron cyclotron resonance (ECR) plasma generator. The N_2 gas (Matheson Tri-gas, 99.9999%) with a flow rate of 20 SCCM and the H_2 gas (Matheson Tri-gas, 99.9999%) with a flow rate of 10 SCCM maintained a pressure of 1.0×10^{-4} Torr throughout 15 min of plasma exposure and 15 min of sample cool-down. A tungsten filament located behind the sample backside was used to heat the samples to 700 °C, and an infrared pyrometer (Mikron, M90-0) was used to measure surface temperature. A microwave power of 300 W was used to ignite the ECR plasma.

III. RESULTS

In this study, we determine the concentrations of external charged surface states from experimentally measured band bending of various Ga-face GaN samples following several dry etch and sample preparation methods.

Samples with no clean prior to XPS measurement exhibited similar band bending measurements of $+0.2 \pm 0.1$ eV regardless of

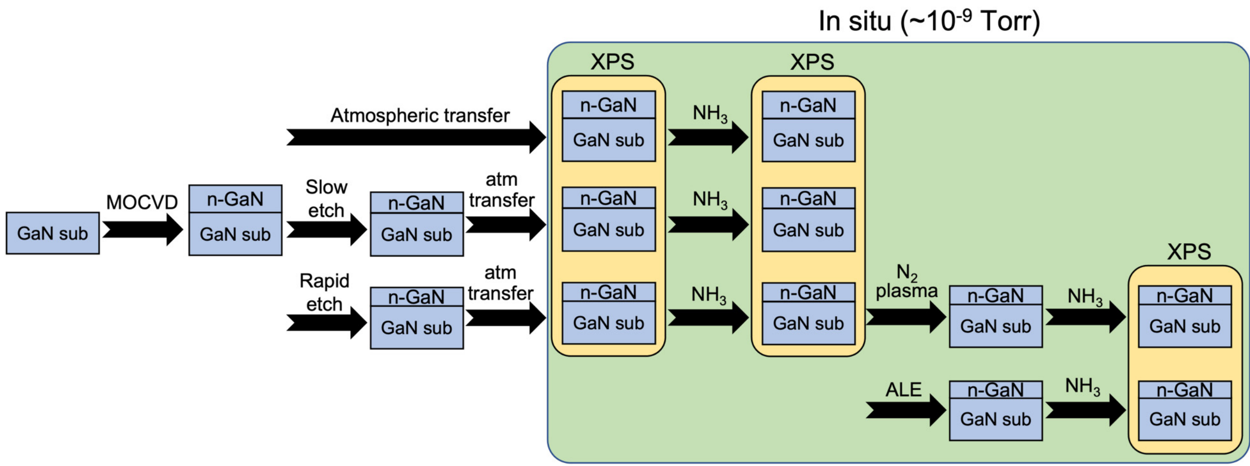

FIG. 5. Process flow of GaN samples throughout growth, etching, processing, and characterization.

Published under an exclusive license by AIP Publishing

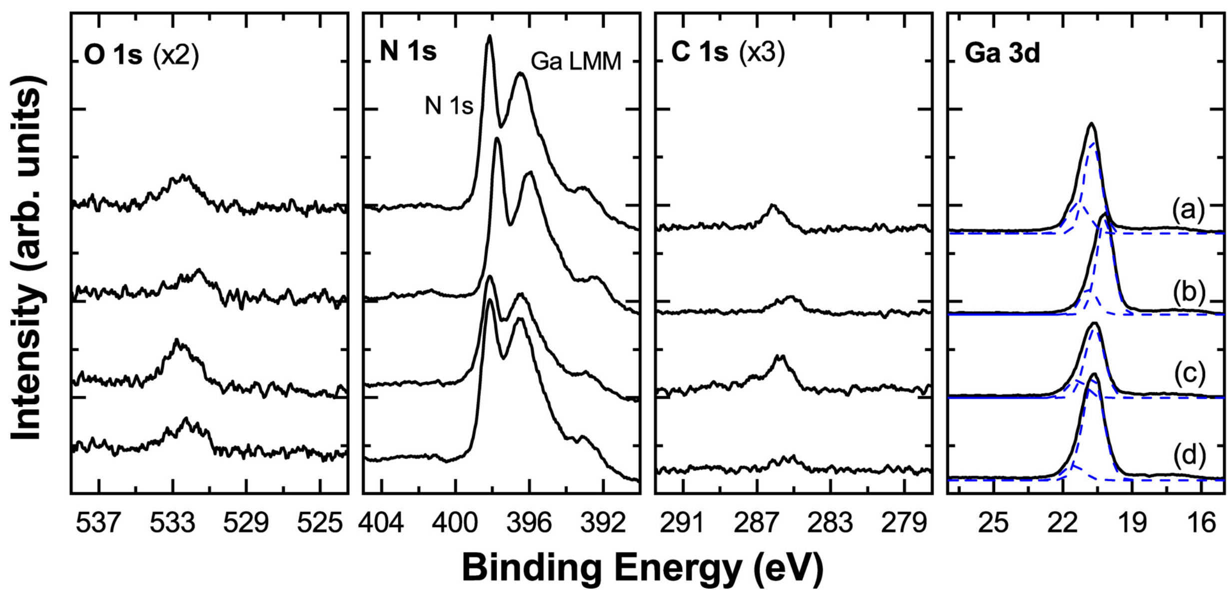

FIG. 6. O 1s, N 1s, C 1s, and Ga 3d XPS scans of GaN under various preparations; including (a) non-etched, (b) *in situ* NH_3 cleaned, (c) rapid ICP etch, and (d) rapid ICP etch with *in situ* NH_3 clean. Ga LMM Auger peaks are also observed to overlap with N 1s.

etch process. This band bending is attributed to surface adsorbates compensating surface charges and thus adsorption-induced band bending dominating the surface. Oxygen and carbon were detected on all surfaces prior to surface cleaning. No other surface impurities were detected by XPS, although another study using secondary ion mass spectroscopy (SIMS) detected Si after ICP etching, likely originating from residual Si in the MOCVD chamber.[60] To remove excessive surface contaminants and produce consistent surface conditions for XPS measurement, samples were cleaned using an *in situ* NH_3 clean at 800 °C for 30 min. Annealing at this temperature in an NH_3 environment may also remove some dry etch related damage; however, this cleaning is necessary to produce consistent surfaces. XPS measurements for all samples after NH_3 surface clean showed increased intensity in Ga 3d and N 1s spectra, while O 1s and C 1s intensity decreased. This is shown for the non-etched and rapid ICP etched GaN in Fig. 6. A Ga LMM Auger peak is also observed to overlap with the N 1s spectra, as indicated in Fig. 6. Shifts in binding energy were observed for these samples after *in situ* cleaning, with a large shift observed for the non-etched sample, shown in Fig. 6. The corresponding change in band bending after the *in situ* cleaning process is listed for the non-etched, rapid ICP etched, slow ICP etched, and ALE samples in Table I.

Intensity of the Ga 3d and N 1s core level XPS peaks of the ICP etched samples were reduced relative to the non-etched GaN. This is attributed to increased surface adsorbates caused by more active surface sites produced by the ICP etch process. Nitrogen deficiency was observed at the surfaces of ICP etched samples with a N:Ga ratio of 0.8 ± 0.2, which is typical of previously reported GaN dry etch methods.[17,19,26] *In situ* cleaning improved the N:Ga ratio of ICP etched samples to 0.9 ± 0.2. *In situ* NH_3 cleaning also reduced O 1s and C 1s intensity, although residual C was detected in some samples after cleaning. Oxygen was not completely removed from the surface as a thin surface oxide was desired for consistent surface termination across all samples while preventing Ga dangling bonds. A significant increase in Ga 3d and N 1s intensities after cleaning was observed in the ICP etched[58,59] as shown in the rapid ICP etch spectra shown in Fig. 6.

Oxygen coverage at the wafer surfaces was defined as the number of adsorbed oxygen atoms at the (0001) surface, where one monolayer (ml) corresponds to one oxygen atom per surface lattice site. The oxygen coverage was calculated from XPS intensities using the relation given in Eq. (8),[61]

$$\Theta_O = \frac{I_O S_{Ga}}{S_0 I_{Ga}} \sum_{n=0}^{\infty} \exp\left[-\frac{n d_{GaN}}{\lambda_{Ga} \cos[\phi]}\right], \quad (8)$$

TABLE I. Change in O coverage and band bending of non-etched and etched GaN following *in situ* NH_3 cleaning.

	O coverage (ml)		Band bending shift after cleaning (eV)
	Initial	Cleaned	
Air exposed	1.2	0.9	+0.6
Rapid ICP etch	2.3	1.1	+0.2
Slow ICP etch	1.8	1.1	+0.3
ALE	2.0	1.3	+0.4

Published under an exclusive license by AIP Publishing

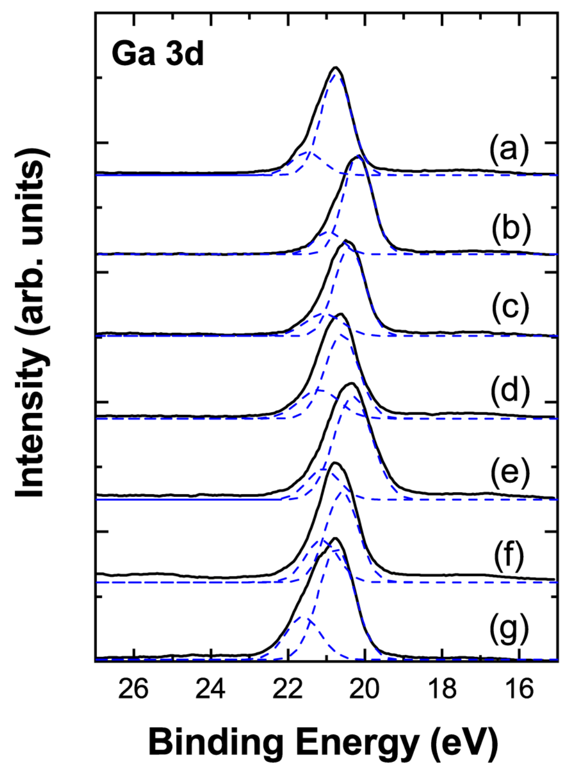

FIG. 7. Band bending was measured using the Ga 3d XPS scans of GaN after various preparations; including (a) air exposed, (b) *in situ* NH_3 cleaned, (c) slow ICP etch, (d) rapid ICP etch, (e) rapid ICP etch and N_2 plasma treatment, (f) rapid ICP etch and ALE, and (g) ALE.

where I_O and I_{Ga} are the integrated intensity of the O 1s and Ga 3d core level peaks; S_O and S_{Ga} are the atomic sensitivity factors for O 1s and Ga 3d electrons (0.66 and 0.31);[55] d_{GaN} is the distance between two GaN planes (2.6 Å); $\phi = 0$ is the photoelectron take-off angle; and $\lambda_{Ga} = 2.4$ nm is the inelastic mean free path of Ga 3d electrons with kinetic energies ~1450 eV, which was calculated using the NIST Electron Inelastic-Mean-Free-Path Database.[62]

The change in O coverage is shown in Table I for GaN following *in situ* NH_3 clean. The *in situ* clean did not fully remove the surface oxide, as was desired to maintain consistent surface termination for all samples. The rapid ICP etch and ALE processes exhibited the highest initial O coverage but were consistent with other O-terminated samples following *in situ* cleaning. Additionally, a change in O content was observed in the FWHM of the Ga 3d spectra. The Ga 3d peak in GaN XPS measurements is broadened when surface oxides are present due to a Ga–O component at the higher binding energy side of the Ga 3d peak. Reduction of the surface oxide results in lower intensity of the Ga–O component and a corresponding reduction of the Ga 3d FWHM. Due to this peak shoulder, deconvolution of the Ga 3d spectra was used to identify the Ga–N 3d peak for band bending calculations.

In addition to O and C, samples etched by ALE also exhibited F at the surface, observed by F 1s and F KLL Auger peaks. ALE samples also exhibited the lowest initial band bending of $+0.0 \pm 0.1$ eV prior to *in situ* cleaning. Band bending of the ALE samples increased to $+0.4 \pm 0.1$ eV following *in situ* cleaning.

The Ga 3d XPS scans are shown in Fig. 7 for *in situ* cleaned, O-terminated surfaces following various etch and processing methods, as well as non-etched, as-received GaN prior to *in situ* cleaning. The non-etched and rapid ICP etch with N_2 plasma treatment exhibited the lowest binding energy, indicating larger upward band bending. The Ga 3d peak of the GaN etched by ALE, shown in Fig. 6(g), exhibited the largest FWHM, which is attributed to broadening by Ga-O and Ga-F peaks at the higher binding energy side.

The band bending determined from XPS measurements is shown in Fig. 8 and Table II. External charge compensation was determined from XPS measurements using Eq. (4) with a GaN donor density of 1×10^{17} cm^{-3}, and the results are also shown in Table II.

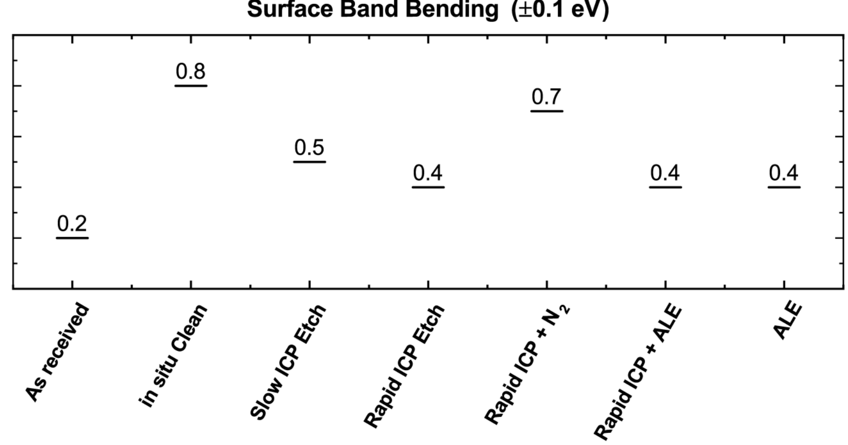

FIG. 8. Band bending measurements of GaN after various ICP etch conditions and surface processing techniques; including as-received (non-etched), *in situ* NH_3 cleaned (non-etched), slow ICP etched, rapid ICP etched, rapid ICP etch with N_2 plasma treatment, rapid ICP etch and ALE, and ALE.

Published under an exclusive license by AIP Publishing

TABLE II. Band bending and external charge concentration of Ga-face GaN (0001) after various etch and surface preparation processes as determined from XPS.

	Band bending (±0.1 eV)	External charge concentration (10^{13} e/cm^2)
Air exposed	+0.2	+1.8
In situ NH_3 clean	+0.8	+1.5
Slow ICP etch	+0.5	+1.6
Rapid ICP etch	+0.4	+1.7
Rapid etch + N_2 plasma	+0.7	+1.5
Rapid etch + ALE	+0.4	+1.7
ALE	+0.4	+1.7

IV. DISCUSSION

Band bending of GaN after various etching and processing methods was determined from XPS measurements of Ga 3d. The effective escape depth of relevant photoelectrons in this study is ~ 5 nm. Measured core level energies, and calculated band structure, using this method are, therefore, an average over the XPS measurement depth. Although XPS penetration depth is unable to directly detect sub-surface ion-related defects, changes in band bending are indicative of underlying material. Correlation between etching and surface processing methods with measured band bending was observed. However, due to a likely inherent Fermi level pinning state located 0.4–0.8 eV below the conduction band,[4,46,48] the measured band bending response is limited. This is attributed to a pinning state able to compensate positive and negative charges. Ga 2p was also observed to experience similar shifts in binding energy for each process. We note that changes in binding energy measured by XPS may also occur due to ion-induced changes to the surface band structure, as well as effects related to fixed charge, surface dipoles, or charging.

The largest band bending was observed for non-etched GaN after *in situ* NH_3 cleaning, which we attribute to lower defect concentration in the surface region, allowing for internal charge compensation and, therefore, lower external surface state formation relative to etched samples. The "slow ICP etch" GaN exhibited higher band bending than the "rapid ICP etch," indicating the lower RF power produced less ion-related damage to the surface and reduced surface state formation in agreement with previous studies of ICP etch-induced damage.[22–26] A large increase in band bending was observed after N_2 plasma exposure for rapid ICP etch GaN. This increase in band bending suggests a decrease in surface state density, which is also in agreement with previous results, indicating that N_2 plasma treatment is effective in the recovery of damage produced by dry etching of GaN.[14–17,27] Despite the ion component of N_2 plasma treatment, previous studies have demonstrated reduced current leakage, which was attributed to suppressed leakage paths and improved surface stoichiometry.[18]

GaN samples etched by a novel ALE method using plasma oxidation, fluorination, and ligand-exchange process exhibited the lowest band bending of 0.0 eV prior to *in situ* cleaning. After cleaning, the ALE samples exhibited a band bending of +0.4 ± 0.1 eV, which is lower than expected and attributed to adsorbed surface contaminants inhibiting upward band bending. Fluorine was observed in XPS measurements accounting for ~3% of surface composition within the XPS detection volume. A slight reduction in F 1s intensity was observed after *in situ* cleaning; however, complete removal of F impurities was not achieved. Post-ALE impurities at the surface may be mitigated by optimization of the etch parameters (particularly substrate temperature and exposure times) or a separate final surface clean could remove the fluorine impurities. The results presented here indicate that the novel ALE process could be appropriate for removal on near-surface etch damage.

V. CONCLUSIONS

XPS core level measurements were used to determine surface band bending of n-type Ga-face GaN (0001) after various dry etching and *in situ* surface preparation methods. External surface charge density arising from compensation of intrinsic spontaneous polarization of GaN was then deduced from band bending measurements. *In situ* cleaning using high temperature NH_3 exposure was used to remove surface contaminants resulting from sample transfer, leaving a thin oxide for consistent surface conditions necessary for band bending comparisons. Increased surface charge density was observed in ICP etched GaN, with surface charge density reduced for GaN etched with lower RF power. N_2 plasma treatment after ICP etching showed increase in band bending and a reduction of the surface charge density, in agreement with previous studies of N_2 plasma treatment effects on etch damage. Determining the work function by UPS may improve this method of measuring surface band bending by identifying effects of surface dipoles and fixed charge.

The results presented here indicate that the novel ALE process described could be appropriate for removal of near-surface etch damage. A separate surface clean to remove residuals from the ALE process may be necessary for specific applications. The use of XPS to evaluate the density of surface states and polarization compensation would be appropriate for developing surface processes for III-nitride materials.

ACKNOWLEDGMENTS

This work was supported by the Advanced Research Projects Agency-Energy through the PN-Diodes program under Grant No. DE-AR0000868. We acknowledge Dr. David Smith, Dr. Fernando Ponce, Dr. Stephen Goodnick, Dr. Xingye Wang, Dr. Mei Hao, Dr. Shanthan Alugubelli, Dr. Hanxiao Liu, Dr. Zhiyu Huang, and Dr. Jesse Brown for their useful discussions. We also acknowledge Dr. Brianna Eller and Dr. Jialing Yang for their initial work in this area.

AUTHOR DECLARATIONS

Conflict of Interest

The authors have no conflicts to disclose.

Published under an exclusive license by AIP Publishing

DATA AVAILABILITY

The data that support the findings of this study are available from the corresponding author upon reasonable request.

REFERENCES

[1]U. K. Mishra, P. Parikh, and Y. F. Wu, "AlGaN/GaN HEMTs—An overview of device operation and applications," Proc. IEEE **90**, 1022 (2002).

[2]B. J. Baliga, "Gallium nitride devices for power electronic applications," Semicond. Sci. Technol. **28**, 1022 (2013).

[3]E. A. Jones, F. F. Wang, and D. Costinett, "Review of commercial GaN power devices and GaN-based converter design challenges," IEEE J. Emerg. Sel. Top. Power Electron. **4**, 707 (2016).

[4]B. S. Eller, J. Yang, and R. J. Nemanich, "Polarization effects of GaN and AlGaN: Polarization bound charge, band bending, and electronic surface states," J. Electron. Mater. **43**, 4560 (2014).

[5]J. A. del Alamo and J. Joh, "GaN HEMT reliability," Microelectron. Reliab. **49**, 1200 (2009).

[6]G. Meneghesso, G. Verzellesi, F. Danesin, F. Rampazzo, F. Zanon, A. Tazzoli, M. Meneghini, and E. Zanoni, "Reliability of GaN high-electron-mobility transistors: State of the art and perspectives," IEEE Trans. Device Mater. Reliab. **8**, 332 (2008).

[7]O. Ambacher, "Polarization induced effects in AlGaN/GaN heterostructures," Acta Phys. Pol. A **98**, 195 (2000).

[8]E. T. Yu, X. Z. Dang, P. M. Asbeck, S. S. Lau, and G. J. Sullivan, "Spontaneous and piezoelectric polarization effects in III–V nitride heterostructures," J. Vac. Sci. Technol. B **17**, 1742 (1999).

[9]S. H. Park and S. L. Chuang, "Spontaneous polarization effects in wurtzite GaN/AlGaN quantum wells and comparison with experiment," Appl. Phys. Lett. **76**, 1981 (2000).

[10]F. Bernardini, V. Fiorentini, and D. Vanderbilt, "Spontaneous polarization and piezoelectric constants of III-V nitrides," Phys. Rev. B **56**, R10024 (1997).

[11]J. Yang, *Interface Electronic State Characterization of Plasma Enhanced Atomic Layer Deposited Dielectrics on GaN* (Arizona State University, 2014).

[12]B. S. Eller, J. Yang, and R. J. Nemanich, "Electronic surface and dielectric interface states on GaN and AlGaN," J. Vac. Sci. Technol. A **31**, 050807 (2013).

[13]K. C. Huang, W. H. Lan, and K. F. Huang, "Inductively coupled plasma reactive ion etching-induced GaN defect studied by Schottky current transport analysis," Jpn. J. Appl. Phys. **43**, 82 (2004).

[14]B. Rong, R. J. Reeves, S. A. Brown, M. M. Alkaisi, E. Van Der Drift, R. Cheung, and W. G. Sloof, "A study of reactive Ion etching damage effects in GaN," Microelectron. Eng. **57–58**, 585 (2001).

[15]Z. Mouffak, A. Bensaoula, and L. Trombetta, "A photoluminescence study of plasma reactive ion etching-induced damage in GaN," J. Semicond. **35**, 3 (2014).

[16]J. M. Lee, K. M. Chang, S. W. Kim, C. Huh, I. H. Lee, and S. J. Park, "Dry etch damage in N-type GaN and its recovery by treatment with an N_2 plasma," J. Appl. Phys. **87**, 7667 (2000).

[17]Z. Mouffak, A. Bensaoula, and L. Trombetta, "The effects of nitrogen plasma on reactive-ion etching induced damage in GaN," J. Appl. Phys. **95**, 727 (2004).

[18]L. Ji-Myon, H. Chul, K. Dong-Joon, and P. Seong-Ju, "Dry-etch damage and its recovery in InGaN/GaN multi-quantum-well light-emitting diodes," Semicond. Sci. Technol. **18**, 530 (2003).

[19]C. R. Eddy and B. Molnar, "Plasma etch-induced conduction changes in gallium nitride," J.: Electron. Mater. **28**, 314 (1999).

[20]Z. Mouffak, N. Medelci-Djezzar, C. Boney, A. Bensaoula, and L. Trombetta, "Effect of Photo-Assisted RIE Damage on GaN," MRS Internet Journal of Nitride Semiconductor Research **8**, 7 (2003).

[21]X. A. Cao, H. Cho, S. J. Pearton, G. T. Dang, A. P. Zhang, F. Ren, R. J. Shul, L. Zhang, R. Hickman, and J. M. Van Hove, "Depth and thermal stability of dry etch damage in GaN Schottky diodes," Appl. Phys. Lett. **75**, 232 (1999).

[22]R. J. Shul, L. Zhang, A. G. Baca, C. G. Willison, J. Han, S. J. Pearton, F. Ren, J. C. Zolper, and L. F. Lester, "High-density plasma-induced etch damage," Mater. Res. Soc. Symp. Proc. **573**, 271 (1999).

[23]R. J. Shul, L. Zhang, A. G. Baca, C. G. Willison, J. Han, S. J. Pearton, K. P. Lee, and F. Ren, "Inductively coupled high-density plasma-induced etch damage of GaN MESFETs," Mater. Res. Soc. Symp. **622**, T751 (2000).

[24]Y. B. Hahn, R. J. Choi, J. H. Hong, H. J. Park, C. S. Choi, and H. J. Lee, "High-density plasma-induced etch damage of InGaN/GaN multiple quantum well light-emitting diodes," J.: Appl. Phys. **92**, 1189 (2002).

[25]R. Qiu, H. Lu, D. Chen, R. Zhang, and Y. Zheng, "Optimization of inductively coupled plasma deep etching of GaN and etching damage analysis," Appl.: Surf. Sci. **257**, 2700 (2011).

[26]R. J. Shul, L. Zhang, A. G. Baca, C. G. Willison, J. Han, S. J. Pearton, K. P. Lee, and F. Ren, "Inductively coupled high-density plasma-induced etch damage of GaN MESFETs," Solid State Electron. **45**, 13 (2001).

[27]D. G. Kent, K. P. Lee, A. P. Zhang, B. Luo, M. E. Overberg, C. R. Abernathy, F. Ren, K. D. Mackenzie, S. J. Pearton, and Y. Nakagawa, "Effect of N_2 plasma treatments on dry etch damage in n- and p-type GaN," Solid State Electron. **45**, 467 (2001).

[28]K. J. Kanarik, T. Lill, E. A. Hudson, S. Sriraman, S. Tan, J. Marks, V. Vahedi, and R. A. Gottscho, "Overview of atomic layer etching in the semiconductor industry," J. Vac. Sci. Technol. A **33**, 020802 (2015).

[29]K. Nojiri, K. J. Kanarik, S. Tan, E. A. Hudson, and R. A. Gottscho, "Atomic Layer Etching: Rethinking the Art of Etch," J. Phys. Chem. Lett. **9**(16), 4814–4821 (2018).

[30]G. S. Oehrlein, D. Metzler, and C. Li, "Atomic layer etching at the tipping point: An overview," ECS J. Solid State Sci. Technol. **4**, N5041 (2015).

[31]S. M. George and Y. Lee, "Prospects for thermal atomic layer etching using sequential, self-limiting fluorination and ligand-exchange reactions," ACS Nano **10**, 4889 (2016).

[32]N. R. Johnson, J. K. Hite, M. A. Mastro, C. R. Eddy, and S. M. George, "Thermal atomic layer etching of crystalline GaN using sequential exposures of XeF_2 and BCl_3," Appl. Phys. Lett. **114**, 243103 (2019).

[33]D. C. Messina, K. A. Hatch, and R. J. Nemanich, Atomic layer etching of gallium nitride enabled by water vapor and O_2-plasma oxidation (unpublished) (n.d.).

[34]S. Porsgaard, P. Jiang, F. Borondics, S. Wendt, Z. Liu, H. Bluhm, F. Besenbacher, and M. Salmeron, "Charge state of gold nanoparticles supported on titania under oxygen pressure," Angew. Chem. Int. Ed. **50**, 2266 (2011).

[35]J. P. Long and V. M. Bermudez, "Band bending and photoemission-induced surface photovoltages on clean *n*- and *p-GaN* (0001) surfaces," Phys. Rev. B **66**, 121308 (2002).

[36]I. Bartoš, O. Romanyuk, J. Houdkova, P. P. Paskov, T. Paskova, and P. Jiříček, "Electron band bending of polar, semipolar and non-polar GaN surfaces," J. Appl. Phys. **119**, 105303 (2016).

[37]R. Huang, T. Liu, Y. Zhao, Y. Zhu, Z. Huang, F. Li, J. Liu, L. Zhang, S. Zhang, A. Dingsun, and H. Yang, "Angular dependent XPS study of surface band bending on Ga-polar n-GaN," Appl. Surf. Sci. **440**, 637 (2018).

[38]Y. Zhao, H. Gao, R. Huang, Z. Huang, F. Li, J. Feng, Q. Sun, A. Dingsun, and H. Yang, "Precise determination of surface band bending in Ga-polar n-GaN films by angular dependent x-ray photoemission spectroscopy," Sci. Rep. **9**, 16969 (2019).

[39]S. J. Cho, S. Dogan, S. Sabuktagin, M. A. Reshchikov, D. K. Johnstone, and H. Morkoc, "Surface band bending in as-grown and plasma-treated n-type GaN films using surface potential electric force microscopy," Appl. Phys. Lett. **84**, 3070 (2004).

[40]S. Chevtchenko, X. Ni, Q. Fan, A. A. Baski, and H. Morkọ, "Surface band bending of a-plane GaN studied by scanning kelvin probe microscopy," Appl. Phys. Lett. **88**, 122104 (2006).

[41]U. Karrer, O. Ambacher, and M. Stutzmann, "Influence of crystal polarity on the properties of Pt/GaN Schottky diodes," Appl. Phys. Lett. **77**, 2012 (2000).

[42]O. Ambacher, R. Dimitrov, M. Stutzmann, B. E. Foutz, M. J. Murphy, J. A. Smart, J. R. Shealy, N. G. Weimann, K. Chu, M. Chumbes, B. Green,

Published under an exclusive license by AIP Publishing

A. J. Sierakowski, W. J. Schaff, and L. F. Eastman, "Role of spontaneous and piezoelectric polarization induced effects in group-III nitride based heterostructures and devices," Phys. Status Solidi B **216**, 381 (1999).
[43]F. Bernardini, V. Fiorentini, and D. Vanderbilt, "Accurate calculation of polarization-related quantities in semiconductors," Phys. Rev. B **63**, 193201 (2001).
[44]W. S. Yan, R. Zhang, Z. L. Xie, X. Q. Xiu, P. Han, H. Lu, P. Chen, S. L. Gu, Y. Shi, Y. D. Zheng, and Z. G. Liu, "A thermodynamic model and estimation of the experimental value of spontaneous polarization in a wurtzite GaN," Appl. Phys. Lett. **94**, 042106 (2009).
[45]J. Lähnemann, O. Brandt, U. Jahn, C. Pfüller, C. Roder, P. Dogan, F. Grosse, A. Belabbes, F. Bechstedt, A. Trampert, and L. Geelhaar, "Direct experimental determination of the spontaneous polarization of GaN," Phys. Rev. B **86**, 081302 (2012).
[46]D. Segev and C. G. Van De Walle, "Origins of Fermi-level pinning on GaN and InN polar and nonpolar surfaces," Europhys. Lett. **76**, 305 (2006).
[47]J. Yang, B. S. Eller, and R. J. Nemanich, "Surface band bending and band alignment of plasma enhanced atomic layer deposited dielectrics on Ga- and N-face gallium nitride," J. Appl. Phys. **116**, 123702 (2014).
[48]T. Hashizume and H. Hasegawa, "Effects of nitrogen deficiency on electronic properties of AlGaN surfaces subjected to thermal and plasma processes," Appl. Surf. Sci. **234**, 387 (2004).
[49]J. R. Waldrop and R. W. Grant, "Measurement of AlN/GaN (0001) heterojunction band offsets by x-ray photoemission spectroscopy," Appl. Phys. Lett. **68**, 2879 (1996).
[50]E. A. Kraut, R. W. Grant, J. R. Waldrop, and S. P. Kowalczyk, *Heterojunction Band Discontinuities: Physics and Device Applications* (Elsevier, New York, 1987).
[51]O. Ambacher, "Growth and applications of group III-nitrides," J. Phys. D: Appl. Phys. **31**, 2653 (1998).
[52]J. Hedman and N. Martensson, "Gallium nitride studied by electron spectroscopy," Phys. Scr. **22**, 176 (1980).
[53]T. E. Cook, C. C. Fulton, W. J. Mecouch, R. F. Davis, G. Lucovsky, and R. J. Nemanich, "Band offset measurements of the GaN (0001)/HfO_2 interface," J. Appl. Phys. **94**, 7155 (2003).
[54]B. S. Eller and R. J. Nemanich, "Surface band bending and interface alignment of plasma-enhanced atomic layer deposited SiO_2 on $Al_xGa_{1-x}N$," J. Appl. Phys. **122**, 125304 (2017).
[55]C. D. Wagner, "Sensitivity factors for XPS analysis of surface atoms," J. Electron Spectrosc. Relat. Phenom. **32**, 99 (1983).
[56]P. Peri, K. Fu, H. Fu, Y. Zhao, and D. J. Smith, "Characterization of as-grown and regrown GaN-on-GaN structures for vertical p-n power devices," J. Electron. Mater. **50**, 2637 (2021).
[57]S. W. King, J. P. Barnak, M. D. Bremser, K. M. Tracy, C. Ronning, R. F. Davis, and R. J. Nemanich, "Cleaning of AlN and GaN surfaces," J. Appl. Phys. **84**, 5248 (1998).
[58]H. B. Profijt, S. E. Potts, M. C. M. van de Sanden, and W. M. M. Kessels, "Plasma-assisted atomic layer deposition: Basics, opportunities, and challenges," J. Vac. Sci. Technol. A **29**, 050801 (2011).
[59]H. C. M. Knoops, T. Faraz, K. Arts, and W. M. M. Erwin Kessels, "Status and prospects of plasma-assisted atomic layer deposition," J. Vac. Sci. Technol. A **37**, 030902 (2019).
[60]K. Fu, H. Fu, X. Deng, P. Y. Su, H. Liu, K. A. Hatch, C. Y. Cheng, D. Messina, R. V. Meidanshahi, P. Peri, C. Yang, T. H. Yang, J. Montes, J. Zhou, X. Qi, S. M. Goodnick, F. A. Ponce, D. J. Smith, R. Nemanich, and Y. Zhao, "The impact of interfacial Si contamination on GaN-on-GaN regrowth for high power vertical devices," Appl. Phys. Lett. **118**, 222104 (2021).
[61]V. M. Bermudez, "Study of oxygen chemisorption on the GaN(0001)-(1×1) surface," J. Appl. Phys. **80**, 1190 (1996).
[62]C. J. Powell and A. Jablonski, *NIST Electron Inelastic-Mean-Free-Path Database*, version 1 (National Institute of Standards and Technology, Gaithersburg, MD, 2010).

Published under an exclusive license by AIP Publishing